EVM Prediction for Massive MIMO

Wael Boukley Hasan, Angela Doufexi, George Oikonomou and Mark Beach
Communication Systems & Networks Group, University of Bristol, U.K.
Email: {wb14488, a.doufexi, g.oikonomou, m.a.beach}@bristol.ac.uk

***Abstract*—Signal to interference plus noise ratio (SINR) is a widely common performance metric used in the majority of massive multiple-input, multiple-output (Ma-MIMO) research. This metric requires prior knowledge of the user channel vectors and the interference caused by inaccurate channel state information (CSI). However, the interference caused by inaccurate CSI can't be calculated for real-world scenarios. On the other hand, a comprehensive performance indicator can be achieved by the Error Vector Magnitude (EVM) metric in real-world scenarios. This considers all impairments upon the transmitted symbol as seen at the receiver. However, measuring the EVM values for a subset of users requires each user to retransmit data symbols. This paper presents an estimation method with high accuracy by associating EVM to SINR values for Ma-MIMO with zero-forcing (ZF) and Minimum Mean Square Error (MMSE). Also introduced is a novel EVM prediction method for subset of users taken from the original set of simultaneous users in a single cell Ma-MIMO. This method jointly relies on the channel correlation between users and the EVM performance to predict the EVM values for a subset of the available users without the need to retransmit data symbols. This method considers the user channel vector and the interference caused by inaccurate CSI, which makes it suitable for Ma-MIMO algorithms, such as user grouping and power control. Real-world experimental data-sets with real-time results are carried out to validate the EVM prediction method using software-defined radio Ma-MIMO testbed.**

***Index Terms*—Massive MIMO, 5G, EVM, SINR estimation**

I. Introduction

Massive multiple-input, multiple-output (Ma-MIMO) is a multi-user (MU) multiple-input, multiple-output (MIMO) architecture with a large number of antennas at the base station (BS) serving several users within the same time and frequency resource [1]. The significant capacity enhancements observations and reporting from various field trials have encouraged the industry to consider Ma-MIMO as key 5G technology for sub-6 GHz wireless access [2] [3]. Theory indicates that the user channel vectors become pairwise orthogonal as the number of BS antennas is increased, facilitating the effective use of matched filtering (MF) [1]. The large number of antennas at the BS affects the MIMO channel by causing a very slow growth in the variance of mutual information compared to its mean. It is shown in [4] that the effects of hardware impairments, small scale fading and noise could also be averaged out by the law of large numbers.

For real system deployments the BS has a fixed number of antennas. The level of spatial orthogonality achieved when using a practical number of antennas in real channels may not be ideal. When the individual user channels become correlated, zero-forcing (ZF) or Minimum Mean Square Error (MMSE) become necessary for reliable data transmission [3] [5]. These linear techniques can suppress the interference between users, but this requires perfect channel state information (CSI). Errors in CSI can occur for many reasons such as local oscillator (LO) phase noise, errors in reciprocity calibration and quantization errors [6]. Although ZF and MMSE algorithms can suppress interference caused by the channel between users and the BS, they are unable to suppress interference caused by inaccuracy in real-time CSI. This raises some challenges that need to be addressed about the signal to interference plus noise ratio (SINR) performance metric used in the majority of Ma-MIMO work. Calculating the SINR value in real-time is not feasible since the interference value caused by inaccurate CSI is unknown.

A common measurement of signal quality used in 3^{rd} Generation Partnership Project (3GPP) long-term evolution (LTE) standards is the Error Vector Magnitude (EVM) [6]. This is a comprehensive metric because it considers all impairments upon the transmitted symbol as seen at the receiver. Therefore, using the EVM metric covers the interference caused by inaccurate CSI. The work in [7] and [8] introduce a relationship between EVM and signal to noise ratio (SNR) performance metrics. This relationship holds for a Single-Input Single-Output (SISO) link or a single-user (SU)-MIMO system. The interference between users in MU-MIMO and Ma-MIMO effect the EVM performance but won't effect the SNR value. The work in [9] replaced the SNR by the SINR to introduce a relationship between SINR and EVM for Ma-MIMO with ZF decoder. This relationship could be used in real-time to estimate the SINR value from the EVM performance. Measuring the EVM value after removing any user requires all the remaining users to retransmit data symbols. Hence relying on the measured EVM to estimate the SINR for a subset of the available users is not applicable. Many user grouping and power control algorithms in Ma-MIMO are based on selecting a subset of the available users and maximising the SINR value. These algorithms can't be applied in real Ma-MIMO system just by relying on the EVM performance.

This paper introduces an estimation method with high accuracy associating EVM to SINR values for massive MIMO with ZF and MMSE. It also introduce a novel EVM prediction method for subset of users taken from the original set of simultaneous users in a single cell Ma-MIMO. An indoor channel, captured from the trial in [3], and independent and identically distributed (IID) Rayleigh channel were used to evaluate the proposed methods in this paper. Two linear decoding techniques are covered: ZF and MMSE. Real-world experimental data-sets with real-time results are carried out to validate the EVM prediction method using software-defined radio massive MIMO testbed.

II. System Model

A single-cell Ma-MIMO architecture is considered in this work. The base station is equipped with a large number of antennas (M) and serves a number of active single-antenna users (K), where ($M \gg$ K). The system operates in time division duplex (TDD) mode and uses the same time-frequency resources for all users. The estimated channel matrix between the users and the BS is denoted by $\hat{\boldsymbol{H}} \in \mathbb{C}^{M\times \mathrm{K}}$. The actual channel matrix used during the uplink data transmission is denoted by $\boldsymbol{H} \in \mathbb{C}^{M\times \mathrm{K}}$, which is given by

$$\boldsymbol{H} = \hat{\boldsymbol{H}} + \boldsymbol{E} \tag{1}$$

where $\boldsymbol{E} \in \mathbb{C}^{M\times K}$ is the difference between the estimated channel and the actual channel used during the uplink data transmission. In this paper the error in the channel estimation between the user equipment (UE) and the BS is modeled as a complex Gaussian distribution $\sim \mathcal{CN}\left(\boldsymbol{0}, \sigma_e^2 \boldsymbol{I}_M\right)$, where $\boldsymbol{I}_M$ is the $M\times M$ identity matrix and σ_e^2 is the error variance [10]. Whilst this model may not be so accurate in reality, it serves to illustrate the potential effects of uplink (UL) CSI inaccuracies in massive MIMO. The equalized UL signal $\hat{\boldsymbol{x}} \in \mathbb{C}^{\mathbb{K}}$ can be expressed as

$$\hat{\boldsymbol{x}} = \boldsymbol{W}(\sqrt{\rho_{ul}}\boldsymbol{H}\boldsymbol{x} + \boldsymbol{n}) \tag{2}$$

where $\boldsymbol{x}$ represents the transmitted symbol vector from all users in the same cell, normalized as $\mathbb{E}\left\{|x_k|^2\right\} = 1$. The corresponding UL transmit power is denoted by ρ_{ul}. Simple UL power control is assumed for the work in this paper. The UL transmit power is adjusted so the received SNR from all users is the same. The additive noise vector is denoted by $\boldsymbol{n}$. The noise variance from the antennas at the BS is modeled as $\sim \mathcal{CN}\left(\boldsymbol{0}, \sigma_n^2 \boldsymbol{I}_M\right)$, where σ_n^2 is the noise variance. $\boldsymbol{W} \in \mathbb{C}^{K\times M}$ is the linear decoder matrix, formed using MMSE, ZF or MF. The impact of inaccurate CSI is illustrated and validated in [11] for UL and downlink (DL) data transmission. The equalized signal for user k can be written as follows:

$$\hat{\boldsymbol{x}}_k = \underbrace{\sqrt{\rho_{ul_k}}\sum_{i=1}^{K}(\boldsymbol{W}\boldsymbol{E})_{k,i}\,\boldsymbol{x}_i}_{\text{Cumulative Error Amplification}} + \overbrace{\sqrt{\rho_{ul_k}}\sum_{i=1}^{K}\left(\boldsymbol{W}\hat{\boldsymbol{H}}\right)_{k,i}\boldsymbol{x}_i}^{\text{Desired Signal + Interference}} + z_k \tag{3}$$

where z_k is the amplified noise for user k. The "Cumulative Error Amplification" part represents the interference introduced by CSI estimation inaccuracies. The interference in the "Desired Signal + Interference" part is caused by the inter-user spatial correlation which can be mitigated by choosing the proper decoder such as ZF.

III. EVM Prediction & SINR Estimation for Massive MIMO

In this section, two different scenarios were considered to evaluate the accuracy of the SINR estimation and the EVM prediction. An IID Rayleigh channel was used in the first scenario with perfect and imperfect CSI, where M=128 and $K \in \{2, 12, 22\}$. In the second scenario, the real channel captured from the trial in [3] was used. The trial took place at the University of Bristol. A patch panel antenna array was setup in a 32×4 to serve 22 user clients in line-of-sight (LOS) and placed 24.8m away with 2.5 wavelength spacing at a 3.51 GHz carrier frequency between users. These scenarios were run through an uplink Ma-MIMO simulator developed at the University of Bristol. In addition to randomly generated channels, new vectors can be transmitted through channels previously captured by the physical system for more extensive analysis. For imperfect CSI in both scenarios, the error in the channel estimation between the UEs and the BS is modeled as a complex Gaussian distribution $\sim \mathcal{CN}\left(\boldsymbol{0}, \sigma_e^2 \boldsymbol{I}_M\right)$ [10] where an error variance of 0.01 (1%) was used for the simulations shown. Whilst this value may be higher or lower and the model may not be so accurate in reality, it serves to illustrate the potential effects of CSI inaccuracies in Ma-MIMO.

A common measurement of signal quality used in 3GPP LTE standards is the EVM [6]. This is a comprehensive metric because it considers all impairments upon the transmitted symbol as seen at the receiver. Higher modulation and coding scheme (MCS) are supported when the EVM is small [12]. From [7] and [12], the EVM can be found as

$$\mathrm{EVM}_{RMS} = \sqrt{\frac{\frac{1}{N}\sum_{n=1}^{N}|S_r(n) - S_t(n)|^2}{\frac{1}{N}\sum_{n=1}^{N}|S_t(n)|^2}} \tag{4}$$

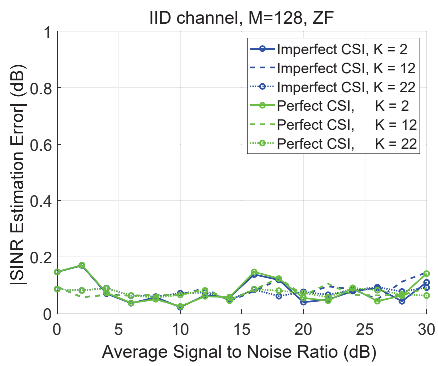

Fig. 1. SINR estimation error using ZF (IID Rayleigh channels).

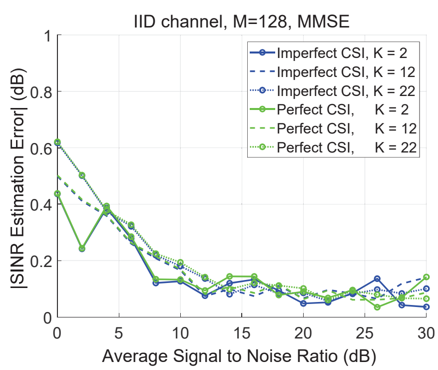

Fig. 2. SINR estimation error using MMSE (IID Rayleigh channels).

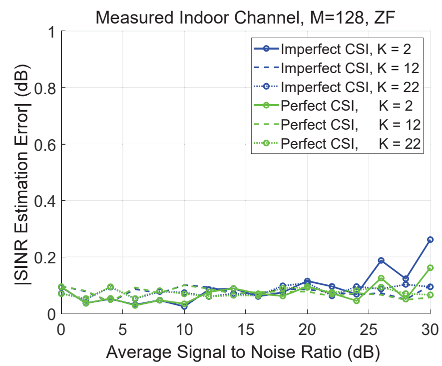

Fig. 3. SINR estimation error using ZF (Measured indoor channels).

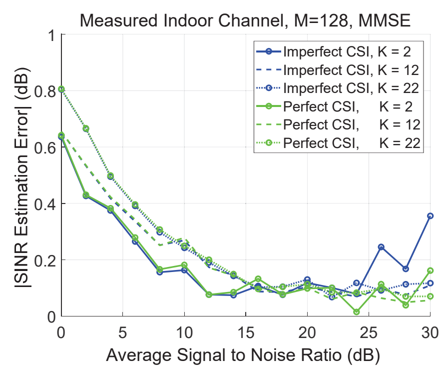

Fig. 4. SINR estimation error using MMSE (Measured indoor channels).

where N is the number of symbols the EVM was measured over. $S_r(n)$ is the nth normalized received symbol and $S_t(n)$ is the ideal value of the n^{th} symbol.

The relation between the EVM and the SNR in a single cell was addressed in many studies such as [7] and [8] which was estimated as follows:

$$\mathrm{EVM}_{RMS}^2 \approx \frac{1}{\mathrm{SNR}} \tag{5}$$

The above approximation can be used in SISO and SU-MIMO. While in MU-MIMO and Ma-MIMO, the interference between users highly impacts the accuracy of this approximation. In order to increase the estimation accuracy, the SINR can be used instead of the SNR as follows:

$$\mathrm{EVM}_{RMS}^2 \approx \frac{1}{\mathrm{SINR}} \tag{6}$$

The accuracy of the above equation can be seen in Fig. 1 and Fig. 2 for the 1st scenario and Fig. 3 and Fig. 4 for the 2nd scenario. The same approximation method was also used in [9]. The UL SINR can be calculated as follows [13]:

$$\mathrm{SINR}_k = \frac{\rho_{ul_k} \left|\boldsymbol{w}_k \boldsymbol{h}_k\right|^2}{\|\boldsymbol{w}_k\|^2 \sigma_n^2 + \rho_{ul_k} \sum_{i\neq k}^{K} \left|\boldsymbol{w}_k \boldsymbol{h}_i\right|^2} \tag{7}$$

The errors in the SINR estimation based on the EVM value from (6) were plotted in Fig. 1 and Fig. 3 using ZF while MMSE was used in Fig. 2 and Fig. 4. When MMSE was used, the SINR estimation error is always below 1 dB. By increasing the SNR above 5 dB, the error in the SINR estimation falls to below 0.4 dB. When ZF was used in both scenarios, the SINR estimation error is always below 0.3 dB.

By selecting a subset of the available users, the UL SINR can be calculated based on the CSI before the data is transmitted from these users (assuming the channel is coherent across the transmission duration); while the EVM can only be measured after the data is transmitted from these users then received and decoded at the BS side. Hence relying on the measured EVM to predict the MCS order for a subset of users is not applicable. Predicting the highest achievable MCS order for each user is essential for selecting the subset of the available users in order to maximize the spectrum efficiency (SE) and provide reliable data transmission. The following two sub-sections III-A and III-B show how the EVM value can be predicted.

A. EVM Prediction Based on SINR Calculation

The UL SINR in (7) is calculated based on perfect CSI. Whilst with imperfect CSI, the equation can be modified

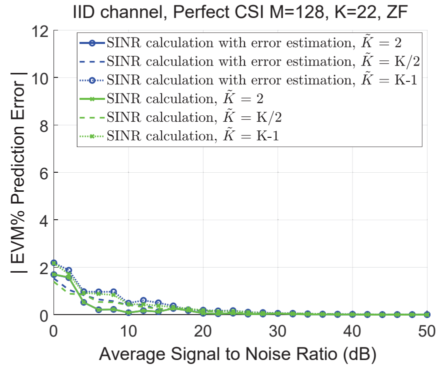

Fig. 5. EVM prediction error with perfect CSI using ZF (IID Rayleigh channels).

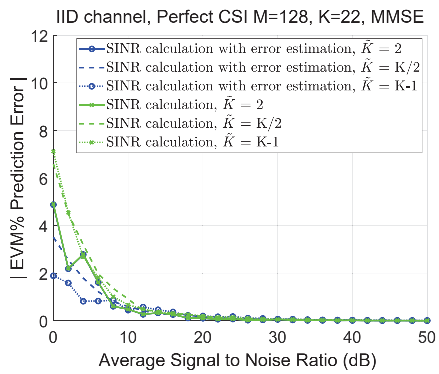

Fig. 6. EVM prediction error with perfect CSI using MMSE (IID Rayleigh channels).

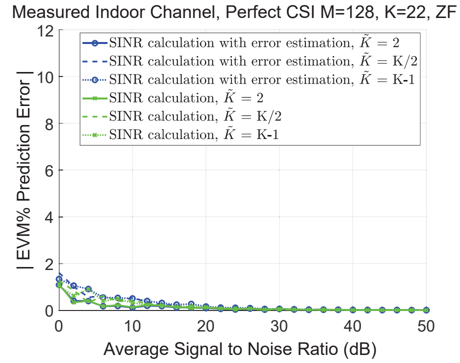

Fig. 7. EVM prediction error with perfect CSI using ZF (Measured indoor channels).

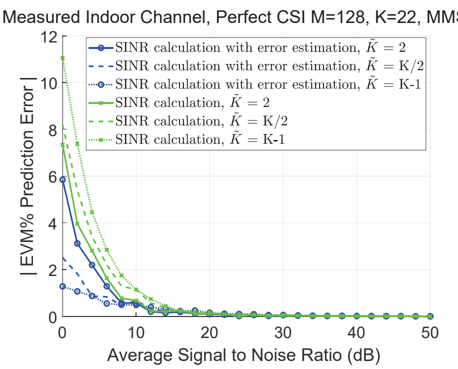

Fig. 8. EVM prediction error with perfect CSI using MMSE (Measured indoor channels).

as follows [14]:

$$\mathrm{SINR}_k = \frac{\rho_{ul_k}\left|\boldsymbol{w}_k\hat{\boldsymbol{h}}_k\right|^2}{\left\|\boldsymbol{w}_k\right\|^2\sigma_n^2 + \rho_{ul_k}\sum_{i=1}^{K}\left|\boldsymbol{w}_k\boldsymbol{e}_i\right|^2 + \rho_{ul_k}\sum_{i\neq k}^{K}\left|\boldsymbol{w}_k\hat{\boldsymbol{h}}_i\right|^2} \tag{8}$$

Since $\boldsymbol{e}$ can't be obtained in real-system, the UL SINR can be estimated by ignoring the error in CSI as follows:

$$\widehat{\mathrm{SINR}}_{\tilde{k}} = \frac{\rho_{ul_{\tilde{k}}}\left|\boldsymbol{w}_{\tilde{k}}\hat{\boldsymbol{h}}_{\tilde{k}}\right|^2}{\left\|\boldsymbol{w}_{\tilde{k}}\right\|^2\sigma_n^2 + \rho_{ul_{\tilde{k}}}\sum_{i\neq\tilde{k}}^{\tilde{K}}\left|\boldsymbol{w}_{\tilde{k}}\hat{\boldsymbol{h}}_i\right|^2} \tag{9}$$

where $\tilde{K}$ is the total number of users in the set that the SINR_k is being predicted for $\left(\tilde{K} \leq K\right)$. From (6), the EVM value for user k can be predicted as follows:

$$\widetilde{\widetilde{\mathrm{EVM}}}^{2}_{RMS_{\tilde{k}}} = \frac{1}{\widehat{\mathrm{SINR}}_{\tilde{k}}} \tag{10}$$

The accuracy of the predicted EVM ($\widetilde{\widetilde{\mathrm{EVM}}}$) square from the above equation is high with perfect CSI. This can be seen in Fig. 5 and Fig. 6 for the 1st scenario and Fig. 7 and Fig. 8 for the 2nd scenario. The green curves show the error between the predicted EVM from (10) before data is transmitted and the actual EVM from (4) after the data is received and decoded. When ZF or MMSE is used, the EVM% prediction error is below 1% at 12 dB SNR (EVM% = $\mathrm{EVM}_{RMS} \times 100$). By increasing the SNR, the EVM% prediction error is reduced until $\widetilde{\widetilde{\mathrm{EVM}}}_{\tilde{k}} = \mathrm{EVM}_k$ at 20 dB SNR.

The accuracy of the CSI in (9) and the number of users can be seen to significantly impact the accuracy of the predicted EVM in (10). This can be seen in Fig. 9 and Fig. 10 for the 1st scenario and Fig. 11 and Fig. 12 for the 2nd scenario. When the SNR is increased above 9 dB and $\tilde{K} = 2$, the EVM% prediction error is always below 1% with ZF and MMSE in both scenarios. When increasing $\tilde{K}$ to 11 $\left(\tilde{K} = K/2\right)$, the EVM% prediction error begins to increase at 20 dB SNR in the 1st scenario and 18 dB SNR in the 2nd scenario. When the SNR value is increased further, the EVM% prediction error is seen to increase as well. The reason for the increment in the EVM% prediction error is the CSI accuracy. The estimated SINR in (9) doesn't consider the interference caused by inaccurate CSI as the interference term embeds the CSI error. Thus, the CSI accuracy has a greater impact on the EVM% prediction

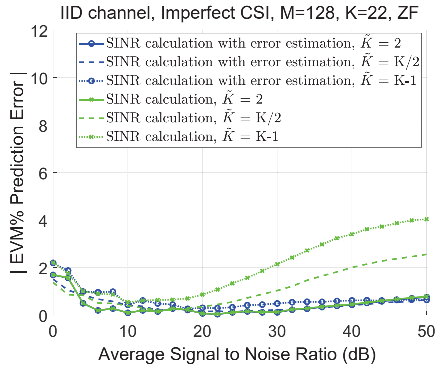

Fig. 9. EVM prediction error with inaccurate CSI using ZF (IID Rayleigh channels).

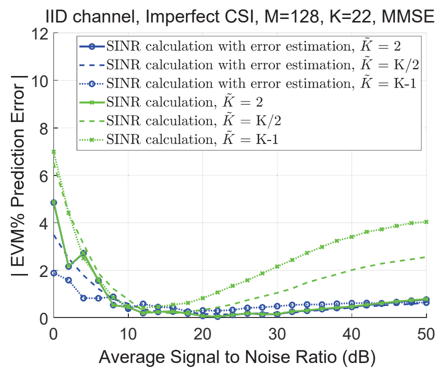

Fig. 10. EVM prediction error with inaccurate CSI using MMSE (IID Rayleigh channels).

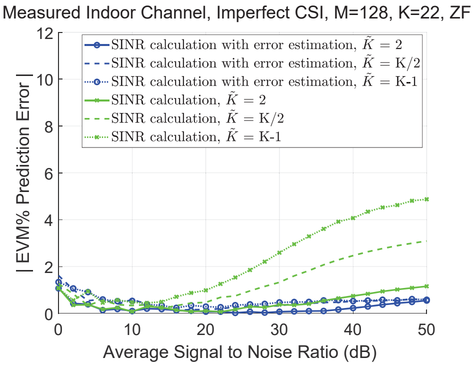

Fig. 11. EVM prediction error with inaccurate CSI using ZF (Measured indoor channels).

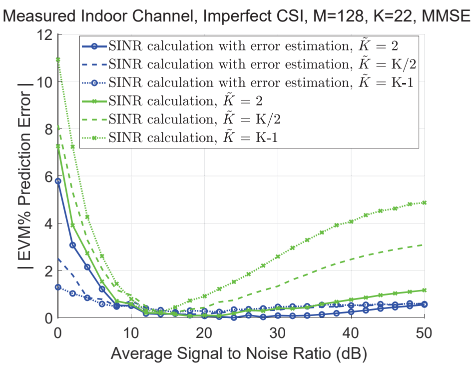

Fig. 12. EVM prediction error with inaccurate CSI using MMSE (Measured indoor channels).

error when the number of users is increased. This can be seen when $\tilde{K}$ is increased to 21 $\left(\tilde{K} = K/2\right)$. The CSI accuracy plays a major role in the EVM prediction based on the SINR calculation method.

B. EVM Prediction Based on SINR Calculation with Error Estimation

The impact of inaccurate CSI is considered in this EVM prediction method. The UL transmit power is adjusted so the received SNR from all users is the same. The EVM value in (4) covers the interference caused by inaccurate CSI, whilst the estimated SINR in (9) does not. So the error caused by inaccurate CSI can be estimated by calculating the SINR value in (9) for user k $\left(\text{when } \tilde{K} = K\right)$ and comparing it with the actual EVM value in (4) as follows:

$$\zeta_k = \left| \mathrm{EVM}^2_{RMS_k} - \frac{1}{\widehat{\mathrm{SINR}}_k} \right| \tag{11}$$

The above error is mainly caused by the inaccurate CSI from all the simultaneous users (the error between SINR and EVM estimation is very small as shown earlier in this section). Since the spatial correlation between users has a significant impact on the interference value, the estimated error in the EVM is divided between users based on the spatial correlation ratio in this method. This can be represented in $\Upsilon \in \mathbb{C}^{K\times K}$ where $\Upsilon_{k,l}$ is the partial EVM^2 error estimation value for user k which is caused only by user l.

$$\Upsilon_{k,l} = \begin{cases} \zeta_k \dfrac{\left|\hat{\boldsymbol{h}}_k^H \hat{\boldsymbol{h}}_l\right|^2}{\sum_{i\neq k}^{K} \left|\hat{\boldsymbol{h}}_k^H \hat{\boldsymbol{h}}_i\right|^2} & \text{if } k \neq l \\ 0 & otherwise \end{cases} \tag{12}$$

After calculating all the partial EVM^2 error estimation values for all the users, the predicted EVM^2 error value for user $\tilde{k}$ (in the subset of $\tilde{K}$ users) can be written as follows:

$$\widetilde{\widetilde{\zeta}}_{\tilde{k}} = \sum_{i=1}^{\tilde{K}} \Upsilon_{\tilde{k},i} \tag{13}$$

By taking into account the above EVM^2 error prediction, equation (10) can be modified as follows:

$$\widetilde{\widetilde{\mathrm{EVM}}}^{\,2}_{RMS_{\tilde{k}}} = \frac{1}{\widehat{\mathrm{SINR}}_{\tilde{k}}} + \widetilde{\widetilde{\zeta}}_{\tilde{k}} \tag{14}$$

The accuracy of the $\widetilde{\widetilde{\mathrm{EVM}}}$ from the above equation is evaluated with perfect CSI and inaccurate CSI. With perfect CSI, this method provides the same accuracy

Fig. 13. Measurement Environment.

Fig. 14. CSN Lab floor plan showing the BS and UEs locations.

as the one in III-A with ZF as shown in Fig. 5 and Fig. 7. When MMSE is used, the proposed method in this section provides higher accuracy compared to the one in III-A. The reason behind this is the low accuracy of the approximation in (6) when MMSE is used with low SNR as shown in Fig. 6 and Fig. 8. Meanwhile, the proposed method in this section has taken into account the difference between the estimated EVM based on the approximation in (6) and the actual EVM from (4).

The main advantage of the proposed EVM prediction method in this section is its high accuracy even with inaccurate CSI and large number of users. This can be seen clearly in Fig. 9 and Fig. 10 for the 1st scenario and Fig. 11 and Fig. 12 for the 2nd scenario. Unlike the EVM prediction method proposed in III-A, this method maintains the EVM% prediction error below 1% when SNR is greater than 8 dB for both scenarios, with ZF and MMSE, even when $\tilde{K}$ is increased from 2 to $K-1$.

IV. Real-Time Validation Using Massive MIMO Test-bed

In this section, we present real-time results from the massive MIMO testbed in [11]. The Communication Systems & Networks (CSN) lab was used for LOS measurements between the BS and 12 UEs from 6 universal software radio peripheral (USRP)s. Measurements were performed outside of university hours and the massive MIMO test-bed was controlled remotely to ensure a static environment was applied in each scenario. An overview of the setup can be seen in Fig. 13. At the BS side, 128 element array was used providing half-wavelength spacing at 3.5 GHz. Three different scenarios were considered in this experiment. UEs were allocated in different places in each scenario, where ZF and MMSE decoders were used. A floor plan of the experiment is shown in Fig. 14 with the UE locations for each scenario. The user identity (ID) of the first UE on the left in Fig. 14 is one. By moving to the right, the user ID is increased by one for each UE.

Fig. 15 shows the EVM values that were displayed in real-time at the BS for all the 12 UEs in the 1^{st} scenario using MMSE decoder. It also shows the users selected by the BS to predict their EVM value after removing 3 users. These results were displayed at ≈ 40 dB SNR from all UEs. The EVM% prediction in Fig. 15 shows the EVM prediction results by using the proposed method in this paper. While the EVM% with perfect CSI in Fig. 15 shows the EVM prediction results assuming a perfect CSI. Fig. 16 shows the EVM values that were displayed in real-time at the BS after removing the 3 selected UEs in Fig. 15. By using the proposed EVM prediction method in this paper, the EVM% prediction error was always less than 1%. The highest EVM% prediction error was 0.74% for user ID 1. While the lowest EVM% prediction error was 0.09% for user ID 8. The same procedures were repeated with ZF and highest EVM% prediction error was 0.69%. When EVM% was calculated based on perfect CSI, the highest EVM% prediction error was 2.7% for user ID 7 and 8.

This experiment was repeated for the 2^{nd} and the 3^{rd} scenarios. By using the proposed EVM prediction method in this paper, the EVM% prediction error was always less than 1%.

V. Conclusion

In this paper, a novel EVM prediction method was proposed for a single cell massive MIMO with ZF and MMSE. This method jointly relies on the channel correlation between users and the EVM performance. The channel correlation provides the interference level before equalizing the signal assuming perfect CSI. While the EVM performance considers the interference from the channel and the interference caused by the inaccurate CSI after equalizing the signal. Channel matrices formed from both IID Rayleigh samples and measured data from

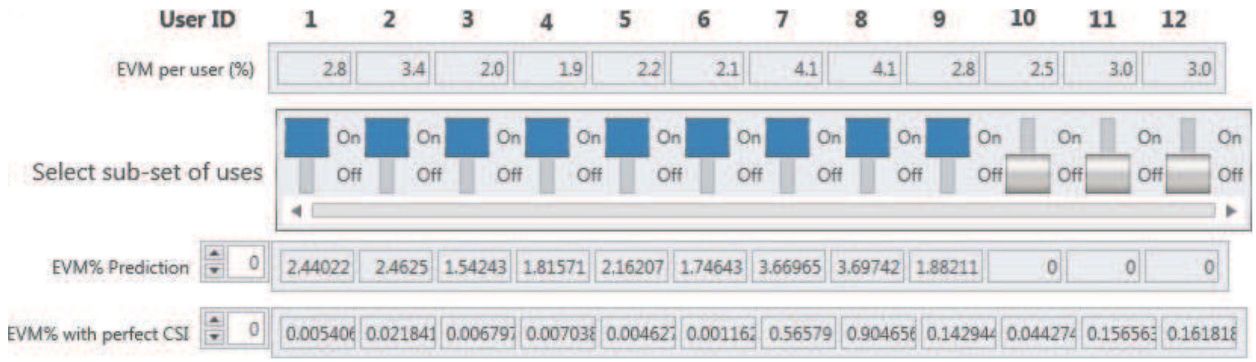

Fig. 15. Captured real-time display for EVM% values from all 12 users, selected UEs for EVM% prediction (9 users), EVM% prediction values for the sub-set of users (9 users) and EVM% with perfect CSI.

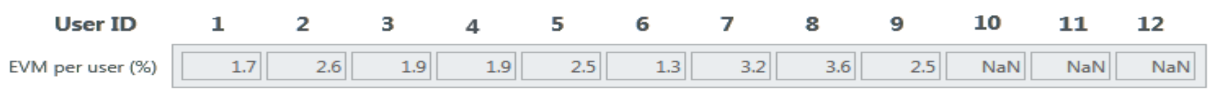

Fig. 16. Captured real-time display for EVM% values for the sub-set of users in Fig. 15 (9 users).

a real Ma-MIMO system were used to evaluate the estimation accuracy. Besides, real-world experimental datasets with real-time results have been used to validated the proposed EVM prediction method. Results from Ma-MIMO simulator show that the EVM% prediction error is less than 1% when SNR is above 8 dB. This was experimentally validated at $\approx$ 40 dB SNR. Furthermore, an estimation method with high accuracy was introduced associating EVM to SINR values for Ma-MIMO with ZF and MMSE.

Acknowledgment

The authors wish to thank Bristol City Council for access to the hardware facility and the financial support from EPSRC TOUCAN (EP/L020009/1) and the EPSRC CDT in Communications (EP/I028153/1) as well as the BBC R&D. Contributions from the University of Lund (Professors Edfors and Tufvesson and their team) alongside that from National Instruments (Nikhil Kundargi and Karl Nieman) in the on-going development of the Massive MIMO Reference Design are most gratefully acknowledged.

References

[1] T. L. Marzetta, "Noncooperative Cellular Wireless with Unlimited Numbers of Base Station Antennas," *IEEE Transactions on Wireless Communications*, vol. 9, no. 11, pp. 3590–3600, nov 2010.

[2] "Facebook Project Aries," 2016. [Online]. Available: https://bit.ly/2OxY5jQ

[3] P. Harris *et al.*, "Serving 22 Users in Real-Time with a 128-Antenna Massive MIMO Testbed," in *2016 IEEE International Workshop on Signal Processing Systems (SiPS)*, Oct 2016, pp. 266–272.

[4] E. G. Larsson, O. Edfors, F. Tufvesson, and T. L. Marzetta, "Massive mimo for next generation wireless systems," *IEEE Communications Magazine*, vol. 52, no. 2, pp. 186–195, February 2014.

[5] T. L. Marzetta, E. G. Larsson, H. Yang, and H. Q. Ngo, *Fundamentals of Massive MIMO* . Cambridge University Press, 2016.

[6] E. Björnson *et al.*, "Massive MIMO Systems With Non-Ideal Hardware: Energy Efficiency, Estimation, and Capacity Limits," *IEEE Transactions on Information Theory*, vol. 60, no. 11, pp. 7112–7139, Nov 2014.

[7] H. A. Mahmoud and H. Arslan, "Error vector magnitude to snr conversion for nondata-aided receivers," *IEEE Transactions on Wireless Communications*, vol. 8, no. 5, pp. 2694–2704, May 2009.

[8] R. A. Shafik, M. S. Rahman, and A. R. Islam, "On the extended relationships among evm, ber and snr as performance metrics," in *2006 International Conference on Electrical and Computer Engineering*, Dec 2006, pp. 408–411.

[9] T. W. C. Brown, D. A. Humphreys, M. Hudlicka, and T. H. Loh, "Prediction of SINR using BER and EVM for Massive MIMO Applications ," in *12th European Conference on Antennas and Propagation*, 2018.

[10] S. Wagner, R. Couillet, M. Debbah, and D. T. M. Slock, "Large System Analysis of Linear Precoding in Correlated MISO Broadcast Channels Under Limited Feedback," *IEEE Transactions on Information Theory*, vol. 58, no. 7, pp. 4509–4537, July 2012.

[11] W. Boukley Hasan *et al.*, "Real-Time Maximum Spectral Efficiency for Massive MIMO and its Limits," *IEEE Access*, vol. 6, pp. 46 122–46 133, 2018.

[12] 3GPP, *TS 36.104 V12.10.0 Release 12*, 2016-01.

[13] Y. S. Cho, J. Kim, W. Y. Yang, and C. G. Kang, *MIMO OFDM Wireless Communication with Matlab*. John Wiley & Sons (Asia) Pte Ltd,, 2010.

[14] T. Bai and R. W. Heath, "Analyzing Uplink SINR and Rate in Massive MIMO Systems Using Stochastic Geometry," *IEEE Transactions on Communications*, vol. 64, no. 11, pp. 4592–4606, Nov 2016.